Comparison of the Magnetic Properties of Metastable Hexagonal Close-Packed Ni Nanoparticles with Those of the Stable Face-Centered Cubic Ni Nanoparticles

Yoon Tae Jeon, Je Yong Moon, and Gang Ho Lee*

Department of Chemistry, College of Natural Sciences, Kyungpook National University, Taegu 702-701, South Korea

Jeunghee Park

Department of Chemistry, Korea University, Jochiwon 339-700, South Korea

Yongmin Chang

Department of Diagnostic Radiology, School of Medicine, Kyungpook National University and Hospital, Taegu 702-701, South Korea

Received: August 16, 2005; In Final Form: November 28, 2005

We report the first magnetic study of pure and metastable hexagonal close-packed (hcp) Ni nanoparticles (sample 1). We also produced stable face-centered cubic (fcc) Ni nanoparticles, as mixtures with the hcp Ni nanoparticles (samples 2 and 3). We compared the magnetic properties of the hcp Ni nanoparticles with those of the fcc Ni nanoparticles by observing the evolution of magnetic properties from those of the hcp Ni nanoparticles to those of the fcc Ni nanoparticles as the number of fcc Ni nanoparticles increased from sample 1 to sample 3. The blocking temperature (T_B) of the hcp Ni nanoparticles is ∼12 K for particle diameters ranging between 8.5 and 18 nm, whereas those of the fcc Ni nanoparticles are 250 and 270 K for average particle diameters of 18 and 26 nm, respectively. The hcp Ni nanoparticles seem to be antiferromagnetic for $T < T_B$ and paramagnetic for $T > T_B$. This is very different from the fcc Ni nanoparticles, which are ferromagnetic for $T < T_B$ and superparamagnetic for $T > T_B$. This unusual magnetic state of the metastable hcp Ni nanoparticles is likely related to their increased bond distance (2.665 Å), compared to that (2.499 Å) of the stable fcc Ni nanoparticles.

1. Introduction

Face-centered cubic (fcc) Ni nanoparticles have been well documented.[1,2] For instance, size-dependent magnetic studies on fcc Ni nanoparticles have shown that both the blocking temperature and the magnetic moment per atom increase with increasing particle size.[2]

Studies of magnetic properties of hexagonal close-packed (hcp) Ni nanoparticles, however, are rare. This is because of the metastability of the hcp structure. Note that the fcc structure is stable for Ni. Early magnetic studies on hcp Ni include those on thin films.[3−6] In those experiments, hcp Ni films were found to be nonmagnetic with a zero magnetic moment at room temperature,[3,5] which is the opposite of ferromagnetic fcc Ni. Recently, hcp Ni nanoparticles have been produced by reducing Ni cations in the solution phase.[7−10] A mixture of hcp and fcc Ni nanoparticles has also been produced by the laser decomposition of nickel carbonyl in the gas phase.[11] The hcp structure changed into the fcc structure upon the application of heat, thus confirming the metastability of the hcp structure at room temperature.[3−5,10] However, note that the metastable hcp structure did not spontaneously decay into the stable fcc structure at room temperature unless the hcp Ni nanoparticles were heated. It is interesting to note that Hinotsu et al. observed a lower magnetization for a mixture of hcp and fcc Ni nanoparticles than for fcc Ni nanoparticles at room temperature, implying that the magnetization of the hcp Ni nanoparticles is lower than that of the fcc Ni nanoparticles.[7]

In this research, we report the first magnetic study of pure and metastable hcp Ni nanoparticles. We also produced stable fcc Ni nanoparticles and compared the magnetic properties of the hcp Ni nanoparticles with those of the fcc Ni nanoparticles. We characterized the magnetic properties by recording both the $M-T$ and $M-H$ curves. We observed that the $M-T$ and $M-H$ curves of the hcp Ni nanoparticles were completely different from those of the fcc Ni nanoparticles. This indicates that the magnetic state of the hcp Ni nanoparticles is different from that of the fcc Ni nanoparticles.

Magnetic states that are different from those of bulk metal have been observed in Fe metal. In fcc Fe films prepared on fcc Cu substrates, both antiferromagnetism and ferromagnetism have been observed.[12−15] Theoretical calculations have also predicted that fcc Fe films could have antiferromagnetism, ferromagnetism, and nonmagnetism, depending on the lattice spacing of the substrates,[16,17] even though the body-centered cubic (bcc) Fe metal, the stable structure at room temperature and 1 atm, is ferromagnetic. Also, note that both MnBi alloy and Heusler alloys (i.e., Cu_2MnSn and Cu_2MnAl), in which none of the elements are themselves ferromagnetic, are ferromagnetic. Slater and Bethe roughly explained ferromagnetism in these alloys such that the Mn atoms are farther apart in alloys than in pure Mn metal and, as a result, spins in Mn atoms become

* Corresponding author. Tel.: -82-53-950-5340. Fax: -82-53-950-6330. E-mail: ghlee@mail.knu.ac.kr.

10.1021/jp054608b CCC: $33.50
Published on Web 12/24/2005

ferromagnetically ordered.[18−20] These examples show that lattice spacing (or bond distance) significantly affects the magnetic state. Note that the bond distance (2.665 Å) of the metastable hcp Ni nanoparticles is much larger than that (2.499 Å) of the stable fcc Ni nanoparticles, as determined in the present work. This indicates that the unusual magnetic properties of the hcp Ni nanoparticles are due to their larger bond distance than that of fcc Ni nanoparticles.

We observed a reduced magnetization in the hcp Ni nanoparticles, compared to that of the fcc Ni nanoparticles. We also observed a sharp phase transition at ∼12 K, which is much lower than that of the fcc Ni nanoparticles at the same particle size. We also observed paramagnetic behavior in the $M-H$ curve at 300 K. These observations, together with nonmagnetism observed in hcp Ni thin films,[3,5] suggest that the hcp Ni nanoparticles might be antiferromagnetic for $T < T_B$ and paramagnetic for $T > T_B$, as discussed in the text. This is very different from the behavior of fcc Ni nanoparticles, which are ferromagnetic for $T < T_B$ and superparamagnetic for $T > T_B$.

2. Experimental Section

2.1. Preparation. The nanoparticles were prepared using a method similar to that of Carturan et al.[10] Instead of using K/B alloy as a reducing agent, however, we used 1.0 M hydrazine in a tetrahydrofuran solvent. We labeled the three samples as samples 1−3, respectively. Two solutions in separate flasks were initially prepared: One is a 8 mL of oleylamine solvent into which 9 mL of hydrazine solution had been added (the reducing agent solution), and the other is 0.15 g of $Ni(acac)_2$ (acac = acetylacetonate) in 10 mL of oleylamine solvent (the precursor solution). All chemicals were purchased from Aldrich and were used as received. During reaction, all solutions were magnetically stirred under a flow of argon gas. Before the precursor solution was injected into the reducing agent solution, both solutions were heated to the same temperature. At a solution temperature of 180 °C, the precursor solution was injected into the reducing agent solution, and the mixture was maintained for 3 h and 30 min (sample 1). For the other samples, the precursor solution was injected into the reducing agent solution at a solution temperature of 90 °C, and this mixture was maintained for 4 h. Then, the solution temperature further increased to 180 °C (sample 2) or 210 °C (sample 3) and maintained for 3 h. All final product solutions were tinted black as a result of nanoparticle formation. After being cooled to room temperature, the solutions were diluted with a mixture of 15 mL of methanol and 15 mL of chloroform. Then, the nanoparticles were separated from the rest of the solution by centrifugation. Note that the metastable hcp Ni nanoparticles did not spontaneously decay into stable fcc Ni nanoparticles at room temperature unless the hcp Ni nanoparticles were heated. This eliminates any change of hcp Ni nanoparticles into fcc Ni nanoparticles during characterization.

2.2. Characterization. The diameters were measured with a transmission electron microscope (TEM) (200 keV, Philips CM 200), the structures were examined with an X-ray diffractometer (XRD) (Philips, X-PERT), and the magnetic properties were evaluated with a Squid magnetometer (Quantum Design, MPMS 7). The average wavelength of the Cu Kα lines, i.e., 1.5418 Å was used for the XRD measurements. The nanoparticles were dispersed in a benzene solvent, and then suspended on copper grids for the TEM measurements. Capsules were sealed with paraffin wax[21] in order to prevent air oxidation after they were filled with Ni nanoparticles for the magnetic property measurements.

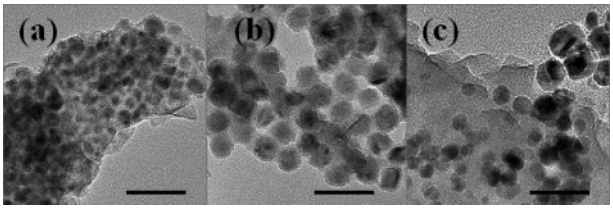

Figure 1. TEM micrographs of (a) sample 1, (b) sample 2, and (c) sample 3. The scale bars represent 50 nm.

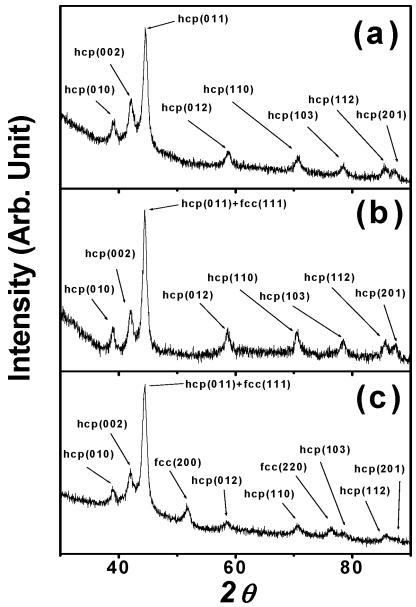

Figure 2. XRD patterns of (a) sample 1, (b) sample 2, and (c) sample 3. The assignments are the Miller indices (*hkl*).

3. Results and Discussion

3.1. TEM Micrographs. Figure 1a−c shows TEM micrographs of samples 1−3, respectively. Here, samples 1 and 2 are nearly monodisperse in diameter with average particle diameters of 8.5 and 18 nm, respectively. Sample 3, however, shows a dual size distribution with average particle diameters of 11 and 26 nm.

3.2. XRD Patterns. Figure 2a−c shows XRD patterns of samples 1−3, respectively.[22] The XRD pattern in Figure 2a seems to show that sample 1 consists of only hcp Ni nanoparticles. This is clearly confirmed by the temperature-dependent magnetization curve ($M-T$ curve), as shown later, in which only the phase transition resulting from the hcp Ni nanoparticles is observed. Although it is not clear for sample 2 from the XRD pattern itself, both samples 2 and 3 consist of hcp and fcc Ni nanoparticles. It is clear that fcc Ni nanoparticles also exist in sample 3 because a separate fcc (200) peak is observed. As confirmed in the $M-T$ curves later, the number of fcc Ni nanoparticles increases from sample 2 to sample 3. The cell constants are estimated to be $a = 2.665$ and $c = 4.300$ Å for the hcp structure and $a = 3.534$ Å for the fcc structure. These cell constants are consistent with the reported values.[1,3−5,10] Note that the bond distances ($2r$ values) estimated from the corresponding cell constants (a values) are 2.499 and 2.665 Å for the fcc and hcp structures, respectively. Thus, the bond distance of the metastable hcp Ni nanoparticles is much larger than that of the stable fcc Ni nanoparticles.

Many studies have shown that the structure of a variety of metallic clusters changes with cluster size (n).[23] This is due to the evolution of stability with n. Although less common, the cluster structure can be affected by production conditions such

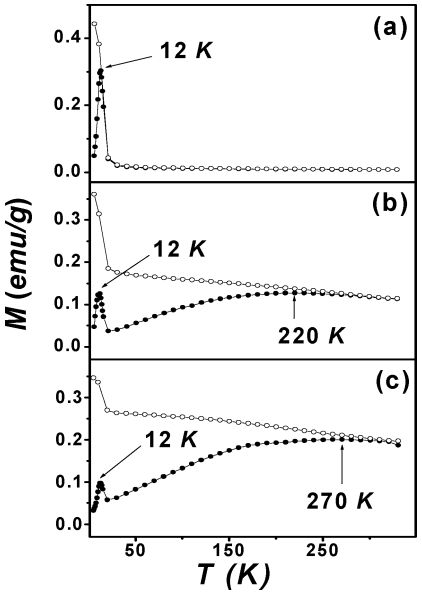

Figure 3. Zero-field-cooled (ZFC) (−●−) and field cooled (FC) (−○− EnDash) magnetization curves versus temperature of (a) sample 1, (b) sample 2, and (c) sample 3.

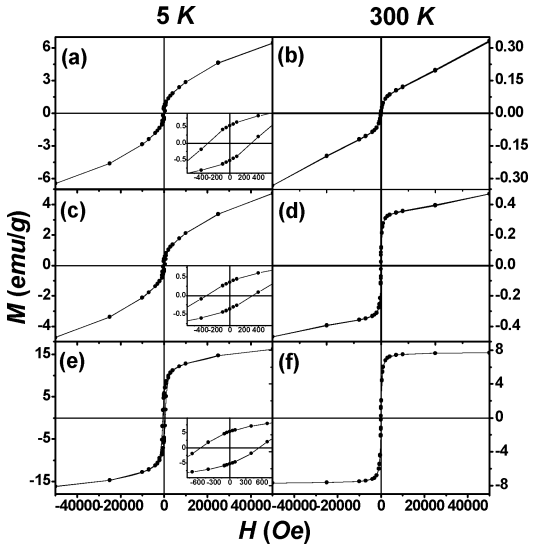

Figure 4. Hysteresis loops of (a,b) sample 1, (c,d) sample 2, and (e,f) sample 3 at 5 and 300 K, respectively. The insets at 5 K are expanded around the origin.

as temperature, pressure, and kinetics. The hcp structure of the Ni nanoparticles is related to the latter case. That is, the hcp Ni nanoparticles were formed under rapid formation conditions, as found in the thermal decomposition of precursors in the polyol process[7] and in laser ablation deposition.[3] In the present experiments, the number of fcc Ni nanoparticles increased with increasing reaction time, thus confirming the metastability of the hcp Ni nanoparticles.

3.3. Magnetic Properties. The magnetic properties of the hcp Ni nanoparticles were studied by recording both the temperature-dependent magnetization ($M-T$) and hysteresis ($M-H$) curves, as shown in Figures 3a−c and 4a−f, respectively. As previously mentioned in the XRD patterns, a single phase transition in the $M-T$ curve for sample 1 clearly shows that this sample consists of only hcp Ni nanoparticles (Figure 3a), whereas two phase transitions in the $M-T$ curves for samples 2 and 3 indicate that both samples consist of hcp and fcc Ni nanoparticles.

From the $M-H$ curves, we estimated the coercivity values (H_c) to be 302, 353, and 546 Oe at 5 K for samples 1−3, respectively. The H_c values, however, are zero at 300 K for all three samples. The $M-T$ curves are composed of zero-field-cooled (ZFC) and field-cooled (FC) curves. From the ZFC curves, we estimated the blocking temperatures (T_B). The T_B values of the hcp Ni nanoparticles were estimated to be ∼12 K for all three samples within the experimental limit. On the other hand, those of the fcc Ni nanoparticles were estimated to be 220 and 270 K for samples 2 and 3, respectively. It is known that T_B generally increases with increasing particle size. This was observed in the fcc Ni nanoparticles.[2] As can be seen in Figure 3, however, T_B of the hcp Ni nanoparticles is nearly the same for average particle diameters ranging between 8.5 and 18 nm. This might indicate that the T_B value of the hcp Ni nanoparticles does not increase much with increasing particle size.

As mentioned with respect to the XRD patterns, the number of fcc Ni nanoparticles increases from sample 1 to sample 3. This can be clearly observed in both the $M-T$ and $M-H$ curves, being more noticeable in the former than in the latter. First, in the $M-T$ curves, the intensity of a sharp peak at ∼12 K, corresponding to the T_B value of hcp Ni nanoparticles, rapidly decreases from sample 1 to sample 3, with respect to the magnetization above 20 K arising from the fcc Ni nanoparticles. Second, in the $M-H$ curves, the loop shape changes from that of the hcp Ni nanoparticles to that of the fcc Ni nanoparticles from sample 1 to sample 3. Thus, both the $M-T$ and $M-H$ curves clearly show that the number of fcc Ni nanoparticles increases from sample 1 to sample 3.

As shown in Figures 3 and 4, both the $M-T$ and $M-H$ curves of the hcp Ni nanoparticles are quite different from those of the fcc Ni nanoparticles. The differences in magnetic properties between the hcp and fcc Ni nanoparticles include the following: First, in the $M-T$ curves, the T_B value of the hcp Ni nanoparticles is much lower than that of the fcc Ni nanoparticles at the same particle size. The blocking temperature (T_B) peak of the hcp Ni nanoparticles is very sharp, whereas that of the fcc Ni nanoparticles is broad. Also, the T_B value of the hcp Ni nanoparticles does not much increase with increasing particle size, whereas that of the fcc Ni nanoparticles does. Second, in the $M-H$ curves, the hcp Ni nanoparticles do not show hysteretic behavior typical for ferromagnetic (or superparamagnetic) materials, whereas the fcc Ni nanoparticles do. Third, in the magnetization curves, the magnetization of the hcp Ni nanoparticles is much smaller than that of the fcc Ni nanoparticles, as shown in Figure 5. Here, the magnetizations of samples 1 and 2 are nearly the same within the experimental limit because sample 2 contains only a small number of the fcc Ni nanoparticles, as revealed from the XRD pattern of sample 2. These results indicate that the magnetic state of the hcp Ni nanoparticles is different from that of the fcc Ni nanoparticles.

Above T_B (≈12 K), the magnetization of the hcp Ni nanoparticles in the $M-T$ curve at an applied field of 100 Oe is nearly zero (Figure 3a). This negligible magnetization can also be observed in the magnetization curve at 300 K (Figure 5b). These are consistent with the zero magnetic moment observed in hcp Ni films at room temperature.[3,5] That is, the hcp Ni films were found to be nonmagnetic.[3,5] In fact, the hcp Ni nanoparticles were not attracted by a laboratory magnet of ∼500 G at room temperature. This indicates that the hcp Ni nanoparticles do not have a ferromagnetic spin structure. This is in contrast to the fcc Ni nanoparticles, which showed a large magnetic moment. Also note that large magnetic moments have also been reported for both icosahedral Ni clusters up to $n = 740$[24] and tetragonal Ni nanoparticles with interstitial oxygens.[25]

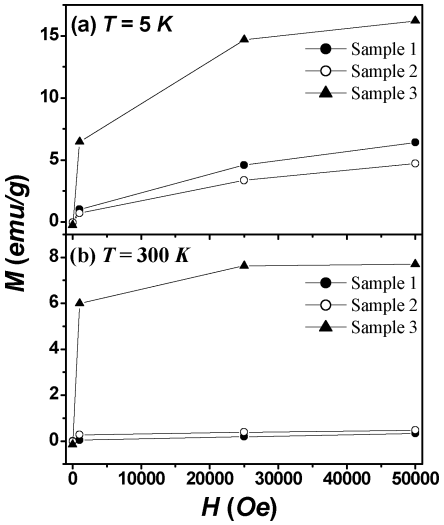

Figure 5. Magnetization curves of sample 1, sample 2, and sample 3 at 5 and 300 K.

From the $M-T$, $M-H$, and magnetization curves, it is clear that the fcc Ni nanoparticles have a ferromagnetic spin structure. That is, the high and zero coercivity values at 5 and 300 K, respectively; the high saturation magnetization; and the hysteretic behavior in the $M-H$ curves clearly show that the fcc Ni nanoparticles are ferromagnetic for $T < T_B$ and superparamagnetic for $T > T_B$, as observed by others.[1,2] On the other hand, we speculate that the hcp Ni nanoparticles are antiferromagnetic for $T < T_B$ and paramagnetic for $T > T_B$, for the following reasons: (1) hcp Ni films were found to be nonmagnetic by other researchers,[3,5] implying that hcp Ni nanoparticles can also be nonmagnetic or antiferromagnetic; (2) the hcp Ni nanoparticles were not drawn by a laboratory magnet of ~500 G, whereas the fcc Ni nanoparticles were strongly drawn, indicating that the hcp Ni nanoparticles are not ferromagnetic; (3) magnetization of hcp Ni nanoparticles was reduced compared to that of fcc Ni nanoparticles (see Figure 5); and (4) in the $M-H$ curve of hcp Ni nanoparticles, antiferromagnetic or paramagnetic behavior was observed except at a low applied field around $H = 0$ Oe (Figure 4a,b), where the low-field region is likely due to uncanceled surface spins. On the basis of these observations, we speculate that the hcp Ni nanoparticles might be antiferromagnetic with T_B at ~12 K. Another point of support for this speculation is the increased bond distance of the hcp Ni nanoparticles, compared to that of the fcc Ni nanoparticles, because at such an enlarged bond distance, a different magnetic state is often observed, as in Fe, where antiferromagnetism is observed.[12,26] Recall that the magnetic state strongly depends on bond distance. The additional hysteretic behavior for a low applied field around $H = 0$ Oe in the $M-H$ curves for the hcp Ni nanoparticles might be due to uncanceled surface spins.

Magnetic states of both metastable and stable structures that have been observed in Fe, Co, and Ni bulk metals, films, and nanoparticles are listed in Table 1. In the case of Co, both hcp and fcc structures are stable at room temperature and 1 atm. Both structures are also ferromagnetic. Note that the bond distances of both structures in Co are nearly the same. This might indicate that the magnetic state is affected not by structure but by bond distance. The magnetic states of metastable structures in both Fe and Ni, however, are quite different from those of the corresponding stable structures. Also, the bond distances of the metastable structures are larger than those of the corresponding stable structures. This shows that the magnetic state is significantly affected by the bond distance. We include the magnetic state of the hcp Ni nanoparticles in Table 1, as speculated from the present and other works.

TABLE 1: Magnetic States, Structures, Cell Constants (a), and Bond Distances ($2r$) of Fe, Co, and Ni Bulk Metals, Films, and Nanoparticles

metal	size	magnetic state	structure	a ($2r$) (Å)
Fe	bulk	ferromagnetic	bcc	2.866 (2.482)[26]
		antiferromagnetic	fcc[a]	3.666 (2.592)[26]
	film	antiferromagnetic	fcc[a]	3.615 (2.556)[12]
		nonmagnetic	fcc[a]	3.439 (2.432)[16]
		ferromagnetic	fcc[a]	3.62 (2.56)[14]
	nanoparticle	ferromagnetic	bcc	2.87 (2.49)[27]
		paramagnetic	fcc[a]	3.615 (2.556)[28]
Co	bulk	ferromagnetic	hcp	2.507 (2.507)[29]
	film	ferromagnetic	hcp	2.49 (2.49)[30]
		ferromagnetic	fcc	3.531 (2.496)[31]
	nanoparticle	ferromagnetic	fcc	3.52 (2.49)[32]
		ferromagnetic	hcp	2.49 (2.49)[33]
Ni	bulk	ferromagnetic	fcc	3.523 (2.491)[34]
	film	nonmagnetic	hcp[a]	2.67 (2.67)[3]
		ferromagnetic	fcc	3.524 (2.491)[3]
	nanoparticle	ferromagnetic	fcc	3.534 (2.499)[b]
		antiferromagnetic[c]	hcp[a]	2.665 (2.665)[b]

[a] Metastable structures at room temperature. [b] Present research. [c] Suggestion of our research.

4. Conclusion

We produced pure and metastable hcp Ni nanoparticles. We also produced stable fcc Ni nanoparticles, as mixtures with the hcp Ni nanoparticles. The magnetic properties of the metastable hcp Ni nanoparticles were investigated, and then they were compared to those of the stable fcc Ni nanoparticles by observing the evolution of magnetic properties from those of hcp Ni nanoparticles into those of fcc Ni nanoparticles as the number of fcc Ni nanoparticles increased. The bond distance (2.665 Å) of the hcp Ni nanoparticles was found to be much larger than that (2.499 Å) of the fcc Ni nanoparticles, which is due to the metastability of the hcp Ni nanoparticles. We observed that the magnetic properties of the hcp Ni nanoparticles were entirely different from those of the fcc Ni nanoparticles. These include (1) the reduced magnetization of the hcp Ni nanoparticles, compared to that of the fcc Ni nanoparticles; (2) the sharp and nearly size-independent blocking temperature (T_B) of the hcp Ni nanoparticles, occurring at ~12 K for particle diameters ranging between 8.5 and 18 nm, whereas those of the fcc Ni nanoparticles are 250 and 270 K for average particle diameters of 18 and 26 nm, respectively; and (3) the antiferromagnetic or paramagnetic behavior of the hcp Ni nanoparticles in the $M-H$ curves, whereas the fcc Ni nanoparticles show ferromagnetic or superparamagnetic behavior. On the basis of these observations and the nonmagnetism observed in the hcp Ni films by other researchers, we speculate that the hcp Ni nanoparticles might be antiferromagnetic for $T < T_B$ and paramagnetic for $T > T_B$. This is very different from the behavior of fcc Ni nanoparticles, which are ferromagnetic for $T < T_B$ and superparamagnetic for $T > T_B$. This unusual magnetic state of metastable hcp Ni nanoparticles is likely related to their increased bond distance (2.665 Å), compared to that (2.499 Å) of the stable fcc Ni nanoparticles, considering that the magnetic state often depends on the bond distance.

Acknowledgment. This work was supported by a Korea Research Foundation Grant funded by the Korean Government (MOEHRD) (KRF-2004-015-C00240).

References and Notes

(1) See, for example: (a) Stepanov, A. L.; Khaibullin, R. I.; Rameev, B. Z.; Reinholdt, A.; Kreibig, U. *Technol. Phys. Lett.* **2004**, *30*, 151. (b)

Rakhimov, R. R.; Jackson, E. M.; Hwang, J. S.; Prokof'ev, A. I.; Alexandrov, I. A.; Karmilov, A. Y.; Aleksandrov, A. I. *J. Appl. Phys*. **2004**, *95*, 7133. (c) Cushing, B. L.; Golub, V.; O'Connor, C. J. *J. Phys. Chem. Solids* **2004**, *65*, 825. (d) Sun, X. *J. Dispersion Sci. Technol*. **2003**, *24*, 557. (e) Pradhan, A. K. *Appl. Surf. Sci*. **2003**, *220*, 26. (f) Zach, M. P.; Penner, R. M. *Adv. Mater*. **2000**, *12*, 878. (g) Host, J. J.; Block, J. A.; Parvin, K.; Dravid, V. P.; Alpers, J. L.; Sezen, T.; LaDuca, R. *J. Appl. Phys*. **1998**, *83*, 793. (h) Jiao, J.; Seraphin, S.; Wang, X.; Withers, J. C. *J. Appl. Phys*. **1996**, *80*, 103. (i) Brunsman, E. M.; Sutton, R.; Bortz, E.; Kirkpatrick, S.; Midelfort, K.; Williams, J.; Smith, P.; McHenry, M. E.; Majetich, S. A.; Artman, J. O.; De Graef, M.; Staley, S. W. *J. Appl. Phys*. **1994**, *75*, 5882.

(2) (a) Ang, K. H.; Alexandrou, I.; Mathur, N. D.; Amaratunga, G. A. J.; Haq, S. *Nanotechnology* **2004**, *15*, 520. (b) Bala, T.; Bhame, S. D.; Joy, P. A.; Prasad B. L. V.; Sastry, M. *J. Mater. Chem*. **2004**, *14*, 2941. (c) Kumar, D.; Yarmolenko, S.; Sankar, J.; Narayan, J.; Zhou H.; Tiwari, A. *Composites B* **2004**, *35*, 149. (d) Cíntora-González, O.; Estournès, C.; Richard-Plouet M.; Guille, J. L. *Mater. Sci. Eng. C* **2001**, *15*, 179. (e) Estournès, C.; Lutz, T.; Happich, J.; Quaranta, T.; Wissler P.; Guille, J. L. *J. Magn. Magn. Mater*. **1997**, *173*, 83.

(3) Vergara, J.; Madurga, V. *J. Mater. Res*. **2002**, *17*, 2099.

(4) Birjega, M. I.; Teodorescu V. S.; Teodorescu, I. A. *Rom. J. Phys*. **1995**, *40*, 919.

(5) Zharkov, S. M.; Zhigalov V. S.; Frolov, G. I. *Phys. Met. Metal*. **1996**, *81*, 170.

(6) Thomson, G. P. *Nature* **1929**, *123*, 912.

(7) Hinotsu, T.; Jeyadevan, B.; Chinnasamy, C. N.; Shinoda, K.; Tohji, K. *J. Appl. Phys*. **2004**, *95*, 7477.

(8) Mi, Y.; Yuan, D.; Liu, Y.; Zhang, J.; Xiao, Y. *Mater. Chem. Phys*. **2005**, *89*, 359.

(9) Illy, S.; Tillement, O.; Machizaud, F.; Dubois, J. M.; Massicot, F.; Fort, Y.; Ghanbaja, J. *Philos. Mag*. **1999**, *79*, 1021.

(10) Carturan, G.; Cocco, G.; Enzo, S.; Ganzerla, R.; Lenarda, M. *Mater. Lett*. **1988**, *7*, 47.

(11) He, Y.; Li, X.; Swihart, M. T. *Chem. Mater*. **2005**, *17*, 1017.

(12) (a) Keune, W.; Halbauer, R.; Gonser, U.; Lauer, J.; Williamson, D. L. *J. Appl. Phys*. **1977**, *48*, 2976. (b) Abrahams, S. C.; Guttman, L.; Kasper, J. S. *Phys. Rev*. **1962**, *127*, 2052.

(13) (a) Würsch, Ch.; Back, C. H.; Bürgi, L.; Ramsperger, U.; Vaterlaus, A.; Maier, U.; Pescia, D.; Politi, P.; Pini, M. G.; Rettori, A. *Phys. Rev. B* **1977**, *55*, 5643. (b) Onodera, A.; Tsunoda, Y.; Kunitomi, N.; Pringle, O. A.; Nicklow, R. M.; Moon, R. M. *Phys. Rev. B* **1994**, *50*, 3532. (c) Johanson, G. J.; McGirr, M. B.; Wheeler, D. A. *Phys. Rev. B* **1970**, *1*, 3208.

(14) (a) Thomassen, J.; May, F.; Feldmann, B.; Wuttig, M.; Ibach, H. *Phys. Rev. Lett*. **1992**, *69*, 3831. (b) Montano, P. A.; Fernando, G. W.; Cooper, B. R.; Moog, E. R.; Naik, H. M.; Bader, S. D.; Lee, Y. C. Darici, Y. N.; Min, H.; Marcano, J. *Phys. Rev. Lett*. **1987**, *59*, 1041.

(15) Pescia, D.; Stampanoni, M.; Bona, G. L.; Vaterlaus, A.; Willis, R. F.; Meier, F. *Phys. Rev. Lett*. **1987**, *58*, 2126.

(16) Marcus, P. M.; Qiu, S. L.; Moruzzi, V. L. *J. Phys.: Condens. Matter* **1999**, *11*, 5709.

(17) (a) Krüger, P. *Phys. Rev. B* **2001**, *64*, 094404. (b) Zhou, Y. M.; Zhang, W. Q.; Zhong, L. P.; Wang, D. S. *J. Magn. Magn. Mater*. **1995**, *145*, L273. (c) Krasko, G. L.; Olson, G. B. *J. Appl. Phys*. **1990**, *67*, 4570. (d) Moruzzi, V. L.; Marcus, P. M.; Kübler, J. *Phys. Rev. B* **1989**, *39*, 6957. (e) Krasko, G. L. *Phys. Rev. B* **1987**, *36*, 8565. (f) Moruzzi, V. L.; Marcus, P. M.; Schwarz, K.; Mohn, P. *Phys. Rev. B* **1986**, *34*, 1784. (g) Pinski, F. J.; Staunton, J.; Gyorffy, B. L.; Johnson, D. D.; Stocks, G. M. *Phys. Rev. Lett*. **1986**, *56*, 2096. (h) Wang, C. S.; Klein, B. M.; Krakauer, H. *Phys. Rev. Lett*. **1985**, *54*, 1852. (i) Bagayoko, D.; Callaway, J. *Phys. Rev. B* **1983**, *28*, 5419.

(18) (a) Slater, J. C. *Phys. Rev*. **1930**, *36*, 57. (b) Slater, J. C. *Phys. Rev*. **1930**, *35*, 509.

(19) Sommerfeld, A.; Bethe, H. In *Handbuch der Physik*; Geiger, H., Scheel, K., Ed.; Springer: Berlin, 1933; Vol. 24-2, p 595.

(20) Cullity, B. D. *Introduction to Magnetic Materials*; Addison-Wesley Publishing Company: Reading, MA, 1972; p 135.

(21) The paraffin wax is antiferromagnetic, and thus, its contribution to the measured magnetic data is negligible.

(22) The 2θ values estimated from the XRD patterns are as follows: Figure 2a: hcp (010) = 39.13°, hcp (002) = 42.15°, hcp (011) = 44.61°, hcp (012) = 58.74°, hcp (110) = 70.68°, hcp (103) = 78.42°, hcp (112) = 85.70°, and hcp (201) = 87.14°. Figure 2b: hcp (010) = 39.01°, hcp (002) = 42.10°, hcp (011) + fcc (111) = 44.49°, hcp (012) = 58.64°, hcp (110) = 70.56°, hcp (103) = 78.44°, hcp (112) = 85.64°, and hcp (201) = 87.14°. Figure 2c: hcp (010) = 39.06°, hcp (002) = 42.06°, hcp (011) + fcc (111) = 44.44°, fcc (200) = 51.74°, hcp (012) = 58.56°, hcp (110) = 70.65°, fcc (220) = 76.35°, hcp (103) = 78.66°, hcp (112) = 85.80°, and hcp (201) = 87.06°.

(23) (a) Tománek, D.; Mukherjee S.; Benneman, K. H. *Phys. Rev. B* **1983**, *28*, 665. (b) Renou A.; Gillet, M. *Surf. Sci*. **1981**, *106*, 27. (c) Gordon, M. B.; Cyrot-Lackmann F.; Desjonquères, M. C. *Surf. Sci*. **1979**, *80*, 159. (d) Oh, S. J.; Huh, S. H.; Kim, H. K.; Park J. W.; Lee, G. H. *J. Chem. Phys*. **1999**, *111*, 7402.

(24) Apsel, S. E.; Emmert, J. W.; Deng, J.; Bloomfield, L. A. *Phys. Rev. Lett*. **1996**, *76*, 1441.

(25) Roy, A.; Srinivas, V.; Ram, S.; De Toro J. A.; Riveiro, J. M. *J. Appl. Phys*. **2004**, *96*, 6782.

(26) Villars, P.; Calvert, L. D. *Pearson's Handbook of Crystallographic Data for Intermetallic Phases*; American Society for Metals: Metal Park, OH, 1985; Vol. 3, p 2162.

(27) (a) Farrell, D.; Majetich, S. A.; Wilcoxon, J. P. *J. Phys. Chem. B* **2003**, *107*, 11022. (b) Veintemillas-Verdaguer, S.; Bomatí, O.; Morales, M. P.; Di Nunzio, P. E.; Martelli, S. *Mater. Lett*. **2003**, *57*, 1184.

(28) Haneda, K.; Zhou, Z. X.; Morrish, A. H.; Majima, T.; Miyahara, T. *Phys. Rev. B* **1992**, *46*, 13832.

(29) Villars, P.; Calvert, L. D. *Pearson's Handbook of Crystallographic Data for Intermetallic Phases*; American Society for Metals: Metal Park, OH, 1985; Vol. 2, p 1736.

(30) Kharmouche, A.; Chérif, S.-M.; Bourzami, A.; Layadi, A.; Schmerber, G. *J. Phys. D: Appl. Phys*. **2004**, *37*, 2583.

(31) Yu, C. C.; Cheng, W. C.; Chen, D. C.; Yao, Y. D.; Liou, Y.; Lee, S. F. *J. Magn. Magn. Mater*. **2002**, *239*, 323.

(32) Petit, C.; Taleb, A.; Pileni, M. P. *J. Phys. Chem. B* **1999**, *103*, 1805.

(33) Lee, G. H.; Huh, S. H.; Oh, S. J.; Kim, B.; Park, J. *J. Korean Phys. Soc*. **2004**, *44*, 1499.

(34) Villars, P.; Calvert, L. D. *Pearson's Handbook of Crystallographic Data for Intermetallic Phases*; American Society for Metals: Metal Park, OH, 1985; Vol. 3, p 2864.